NANOMATERIALS SCIENCE & ENGINEERING
Vol. 2, No. 4, pp. 148-153 (2020)

RESEARCH ARTICLE

https://doi.org/10.34624/nmse.v2i4.19557

Improved performance of Silicon solar cells by ZnMgO front layer

Amel Bahfir *, Messaoud Boumaour, Zoubir Chaieb, Hadjira Labeche

DDCS / Research Centre in Semiconductor Technology for Energetics (CRTSE). 2, Bd. Frantz Fanon, B.P. 140 -7 Merveilles, Algiers, Algeria
**Corresponding author, e-mail address: bahfir.amel@yahoo.fr, a.bahfir@crtse.dz*

Received 22 July 2020; accepted 1 December 2020; published online 15 December 2020

ABSTRACT

Silicon solar cells play a dominant role in the photovoltaic market. However, their manufacturing process is quite expensive and involves complex processes. Therefore, new materials are intensively explored for the aim of potentially higher efficiency and lower cost solar cells.

ZnMgO alloy is a very promising transparent conductive oxide layer and which acts as front layer as well as an anti-reflective coating in silicon solar cells reducing costs and complexity of process.

Numerical simulation using the SCAPS-1D software enables to find the optimized parameters of p-Si/ZnMgO hetero-junction in comparison with the structure comprising ZnO front layer. Even with the effect of stress caused by the high lattice mismatch at the ZnMgO/Si interface, our calculations show a conversion efficiency of 16.57%. Introduction of a thin layer of hydrogenated amorphous silicon improves the cell output performance to 17.14%.

1. INTRODUCTION

The main energy sources used today are fossil fuels, which represent more than 80% of current global primary energy demand, but their increasing consumption has led to serious environmental pollution and global warming [1, 2]. Solar energy, which is totally inexhaustible and sustainable has a double benefit: environmentally friendly and low cost energy sources [3, 4]. Since 2000 to 2013, the mean annual installation of solar panels increased by 48% [5].

Silicon-based solar cells play dominate role in production technology for electricity from sunlight [6]. They are prepared from either multicrystalline (mc-Si), crystalline (c-Si) or amorphous (a-Si) silicon substrates. The best silicon solar cell, developed by Kaneka Corporation, is able to achieve a conversion efficiency of 26.7% [7, 8]. However, the cells with best performance requires a very high cost and complicated processing techniques to reduce cost and improve the manufacturing process. Recently, major work has been proposed to produce low cost devices using thin film technology [9, 10]. Recent research shows that the use of a transparent conductive oxide (TCO) on the front face with the silicon substrate facilitates the transport of charge carriers from the active layer to the metallic contact [11]. Among several TCO materials available, ZnO that is still under development has become a suitable front layer material due to the better optical and electrical properties [12].

The use of the ZnMgO alloy as TCO will further improve performance. Indeed, at low concentrations of Mg, ZnMgO has similar properties to ZnO with the advantage of being able to adjust the band gap with different levels of Mg content. The increase of Mg content increases the band gap from 3.2 to 3.9 eV. With a wider band gap, more incident light in the short wavelength region can be absorbed in the absorber layer. Furthermore, the interface between the front and absorbent layers can be adjusted appropriately by

adjusting the Mg / (Zn + Mg) ratio thus creating an optimal band alignment, which improves the transport of charge carriers [13].

2. DEVICE SIMULATION DETAILS

This new model of Si-based single heterojunction solar cells is modelled using the simulator SCAPS-1D (Solar Cell Capacitance Simulator - version 2.9.4) developed at the University of Gent [14]. It is based on the numerical resolution of the basic semiconductor device equations: Poisson equation as well as the hole and electron continuity equations, completed with appropriate boundary and limit conditions.

The parameters of each material used in the numerical simulation are presented in table 1. They have been carefully selected, based on data extracted from either experimental or other published values [15-17]. All numerical simulations for this work uses a surface recombination velocity of 10^7cm/s, which corresponds more or less to the thermal agitation speed of the electrons [18]. AM1.5G illumination spectrum (incident light power 1000 W/m^2) was used as the incident light source based on the standards of the American Society for Testing and Materials (ASTM). The operating temperature was set to 300K.

ZnO front layer presents a disadvantageous lattice mismatch (> 40%) at the interface between ZnO and Si(100) which leads to high interfacial defect density ($5x10^{14}$ cm^{-2}). When replacing ZnO by a $Zn_{1-x}Mg_xO$ alloy, the lattice constant of a-axis in the $Zn_{1-x}Mg_xO$ increases slightly with increasing Mg content, which slightly decreases the lattice mismatch at the Si/$Zn_{1-x}Mg_xO$ interface.
This study was carried out for low Mg concentrations. Therefore, a slightly lower interfacial defect density was considered ($1x10^{14}$ cm^{-2}).

3. RESULTS AND DISCUSSION

Several studies show that ZnO grown on Si is one of the inexpensive alternatives that can act both as an active n layer and as anti-reflection coating [16]. However, the poor lattice mismatch and high conduction band offset at the Si/ZnO interface are known to degrade the performance of cells.

Table 1. Baseline Values of Physical Parameters.

Material properties	**p-Si**	**i-a-Si**	**n-ZnO**	**n-$Zn_{1-x}Mg_xO$**
Layer Thickness (nm)	2.00E+5	5	2.00E+2	2.00E+2
Relative permittivity $\varepsilon/\varepsilon_0$	11.90	11.90	7.80	8.75
Electron mobility μn (cm^2/V.s)	1.04E+3	20	1.00E+2	1.00E+2
Hole mobility μp (cm^2/V.s)	2.5 E +1	5	2.50 E +1	2.50E +1
Acceptor concentration (1/cm^3)	2.0E+16	0	0	0
Donor concentration (1/cm^3)	0	0	1.0E+19	1.0E+19
Effective density of state N_c (1/cm^3)	2.8E+19	1.00E+20	2.22E+18	2.22E+18
Effective density of state N_v (1/cm^3)	1.04E+19	1.00E+20	1.8E+19	1.8E+19
Band gap E_g (eV)	1.12	1.72	3.3	3.208+1.509x
Electron affinity χ (eV)	4.05	3.9	4.5	4.6+0.16-1.056x

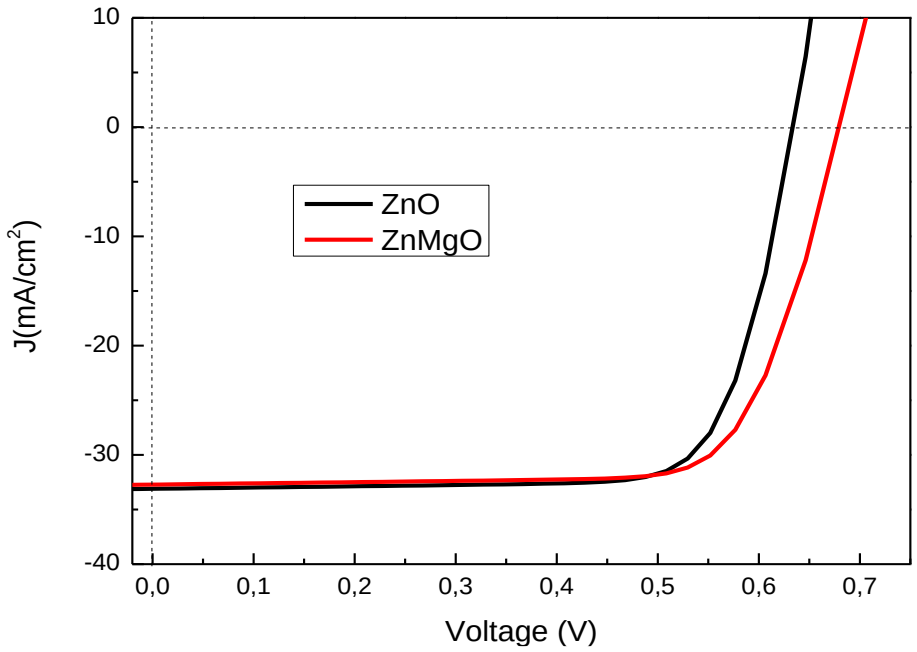

Figure 1. I-V curve of Si/ZnO compared to Si/ $Zn_{0.8}Mg_{0.2}O$.

Replacing ZnO by ZnMgO provides a significant improvement in the band alignment at the p-n heterojunction and a slight decrease in lattice mismatch thanks to appropriate adjustment of the Mg concentration of ZnMgO ternary alloy.

A comparative study of both structures has been carried out. Figure 1 presents the I-V curve of

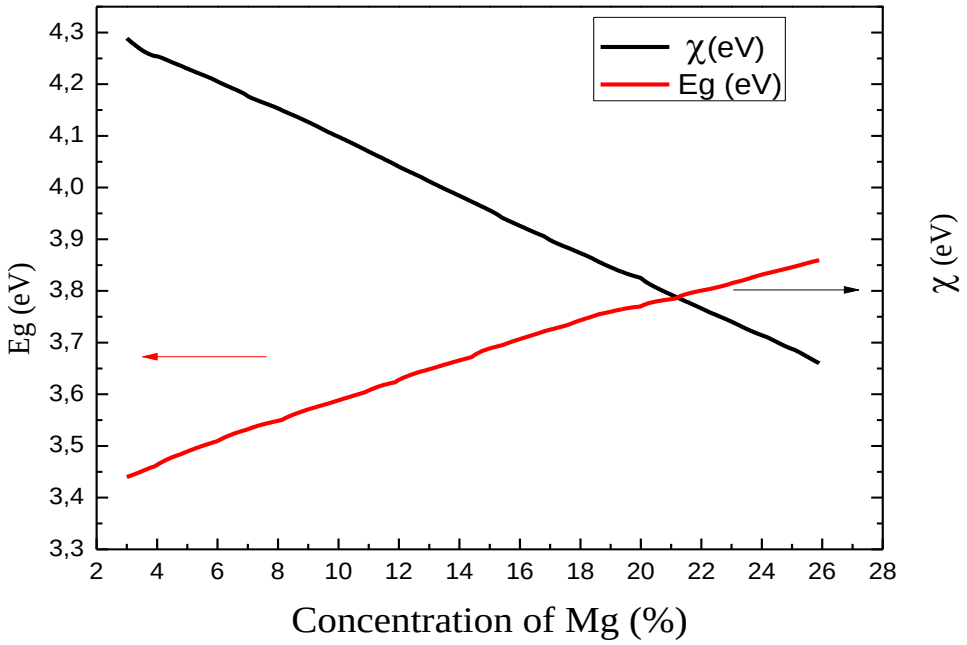

Figure 2. Band gap and electronic affinity as a function of the Mg content of ZnMgO.

Si/ZnO compared to Si/ZnMgO with 20% Mg. The results show almost similar J_{sc} values but the open-circuit Voltage (V_{oc}=635.1 mV) is lower than that of the Si/ZnMgO structure (V_{oc}=655.0 mV) which leads to a relative lower conversion efficiency (η= 16.10%), compared to 16.57% for Si/ZnMgO.

The effect of conduction and valence band offset (CBO, VBO) at the interface of ZnMgO/Si layers on output performance, have been theoretically studied. In fact, the optimization of the conduction/valence band offset in Si-based solar cells makes it possible to reduce the recombination of charge carriers.

The electron affinity (χ) and bandgap (E_g) variation of ZnMgO as a function of the Mg content is shown in figure 2. These values have been chosen based on literature where ZnMgO is used as a window layer in CIGS-based solar cells [19].

To keep the wurtzite phase, one should consider an Mg content below 30%. This is because of several experimental studies have argued that it can be considered as an upper limit due to the thermodynamic solubility limit of MgO in ZnO which is caused by precipitation of the secondary phases [20].

Variations of CBO and VBO at interface between Si and ZnMgO depending on the alloy composition are shown in figure 3.

The presence of a band offset in the form of a "spike" or a "cliff" results in an increase in the recombination current at the interface thus inducing a reduction in the conversion efficiency. This band offset is strongly influenced by the width of the bandgap and the electronic affinity of ZnMgO and Si. These two parameters are controlled by the Zn / Mg ratio.

The discontinuity in the conduction and valence band edges are given by:

$$\Delta E_c = \chi_{\mathrm{Si}} - \chi_{\mathrm{ZnMgO}} \quad (1)$$

$$\Delta E_{\mathrm{v}} = \chi_{\mathrm{ZnMgO}} - \chi_{\mathrm{Si}} + (E_{g\ \mathrm{ZnMgO}} - E_{g\ \mathrm{Si}}) \quad (2)$$

Where ΔE_c, ΔE_v are conduction and valence band edge discontinuities, χ is electron affinity.

Figure 4 shows the detailed effects of Mg content on cell performance parameters. At the low concentration of Mg, V_{oc}, fill factor (FF) and short circuit current (J_{sc}) increase depending on the composition of the alloy and then remains almost stable beyond x = 40%. The optimum Mg concentration is found at 20%.

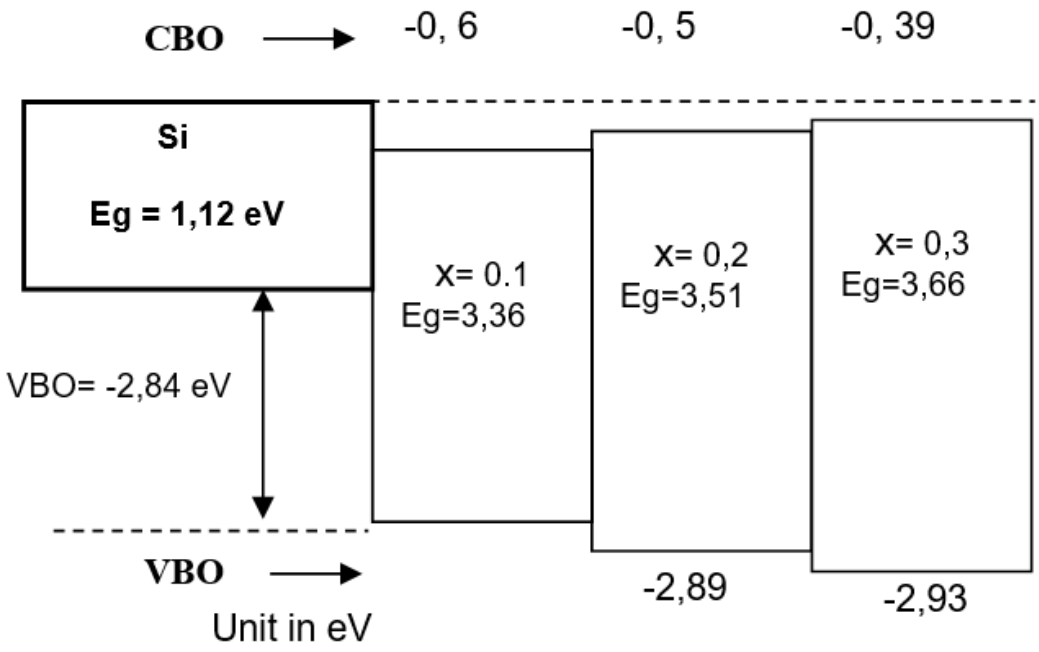

Figure 3. Band alignment at the Si/ $Zn_{1-x}Mg_xO$ interface with different Mg concentration.

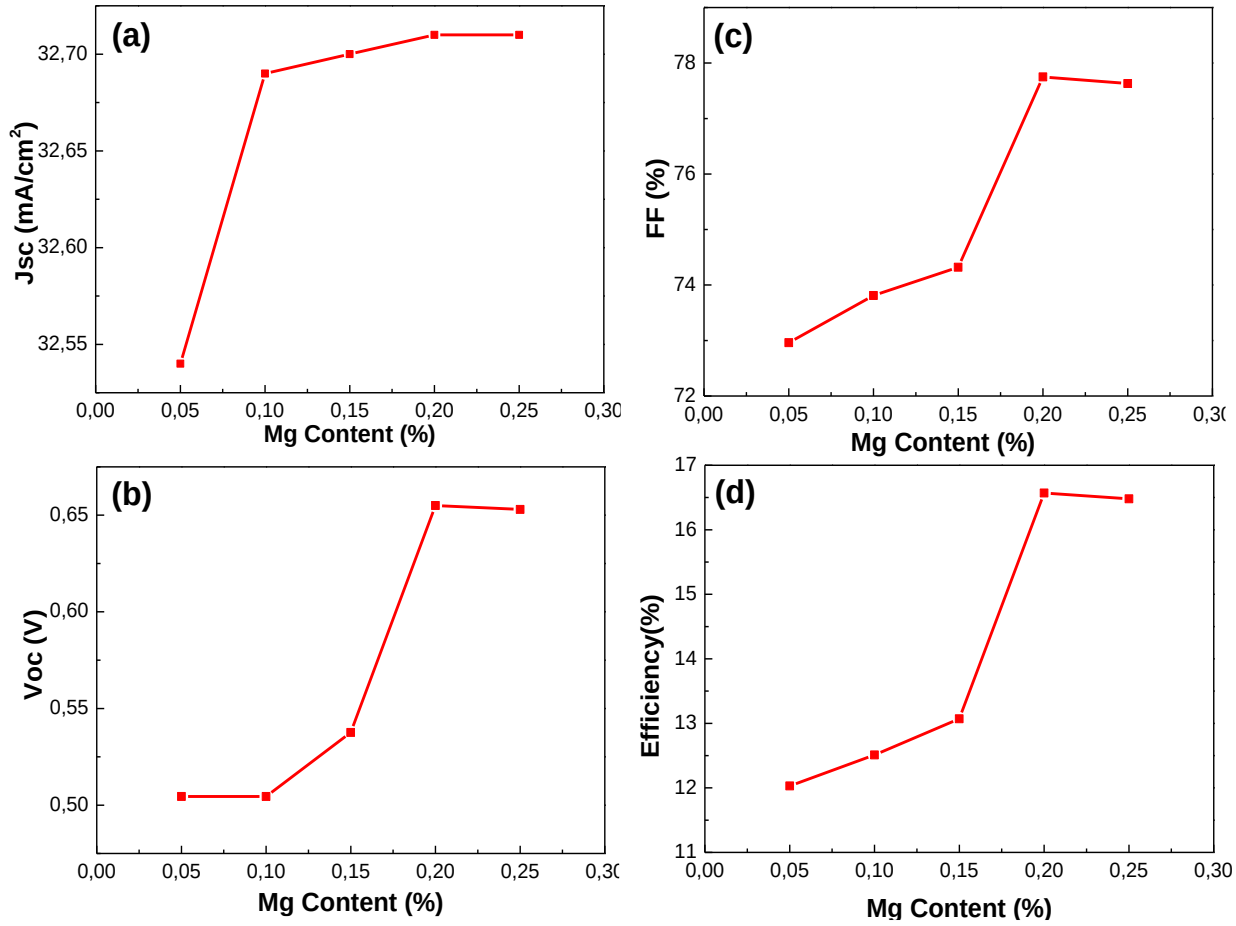

Figure 4. Performance of Si/ $Zn_{1-x}Mg_xO$ cell with different Mg concentrations:
(a) short circuit current , (b) open circuit voltage, (c) fill factor FF and (d) Conversion efficiency.

Although the CBO has a good band alignment, a slight degradation of performance is obtained beyond 25% due to the large VBO caused by widening of the bandgap of ZnMgO. The inclusion of a lower passivation layer using intrinsic silicon (i:a-Si) between Si and ZnMgO improves interface quality. Its optimal bandgap between the two hetero-interfaces can slow down the photon-generated carrier recombination and induces a higher V_{oc} and J_{sc}, hence improved efficiency.

Table 2 summarizes the output performance of the Silicon solar cells with the different layers investigated in this work. similar efficiencies have been obtained for silicon structures with TCO layer [21].

Table 2. The simulated output performance for different structures.

Structure	V_{oc}(mV)	J_{sc}(mA/cm^2)	FF (%)	η (%)
Si/ZnO	635.1	33.11	76.57	16.10
Si/ZnMgO	655.0	32.54	77.57	16.57
Si/i-a-Si/ZnMgO	665.7	33.12	77.78	17.14

4. CONCLUSION

In summary, a comparative study of ZnO and ZnMgO front layers in Si-based solar cells have been analysed using Capacitance Simulator SCAPS-1D. The Mg content effect on conduction and valence band offset at the interface of ZnMgO/Si layers has been theoretically analysed. For a Mg concentration of 20%, the results demonstrate an optimal performance and an improvement relative to the pure ZnO. Cell performance is also closely related to interface defect states. The introduction of a thin intrinsic amorphous silicon layer significantly improves the cell output performance to 17.54%.

ACKNOWLEDGEMENTS

This work was funded under the Algerian General Directorate of Scientific Research and Technological Development (DGRSDT). Authors wish to acknowledge Marc Burgelman, University of Gent, Belgium for his kind provision of the SCAPS-1D solar cell simulator.

REFERENCES

[1] N. Abas, A. Kalair, N. Khan, *Futures* **69**, 31- 49, (2015)
[2] D. Gielen, F. Boshell, D. Saygin, M. D. Bazilian , N. Wagner, R. Gorini, *Energy Strategy Reviews* **24**, 38-50, (2019),
[3] [A. Chel, G. Kaushik, *Alexandria Engineering journal* **57(2)**, 655-669, (2018).
[4] D.N.F. Muche, S.A. Carminati, A. F. Nogueira, F. L. Souza, *Solar Energy Materials and Solar Cells* **208**, 1037, (2020).
[5] A. Rawat, M. Sharma, D. Chaudhary, S. Sudhakar, S. Kumar, *Solar Energy* **110**, 691–703, (2014).
[6] M.R. Sabour, M.A. Jafari, S.M.H. Gohar, *Silicon*, **12**, 2705-2720 (2020).
[7] M. A. Green, E.D. Dunlop, J. Hohl-Ebinger, M. Yoshita, N. Kopidakis, & A.W.Y. Ho-Baillie, *Progress in Photovoltaics: Research and Applications*, **28(1),** 3–15, (2020).
[8] K. Yoshikawa, H. Kawasaki, W. Yoshida, T. Irie, K. Konishi, K. Nakano, T. Uto, D. Adachi, M. Kanematsu, H. Uzu, K. Yamamoto, *Nature Energy*, **2(5),** 17032, (2017).
[9] R. Pietruszka, B.S. Witkowski, E. Zielony, K. Gwozdz, E. Placzek-Popko, M. Godlewski, *Solar Energy*, **155**, 1282–1288, (2017).
[10] S. Chala, N. Sengouga, F. Yakuphanoğlu, S. Rahmane, M. Bdirina, I. Karteri, *Energy* ,**164**, 871-880, (2018).
[11] F. Z. Bedia, A Bedia, M. Aillerie, N. Maloufi, F. Genty, B. enyoucef, *Energy Procedia*, **50**, 853–861. (2014).
[12] B. Hussain, A. Ebong, I. Ferguson, IEEE 42nd Photovoltaic Specialist Conference (PVSC), 15664803, (2015).
[13] A. Bahfir, M. Boumaour, M. Kechouane, Optik, 169, 196–202, (2018).
[14] M. Burgelman, K. Decock, S. Khelifi, A. Abass, *Thin Solid Films* **535**, 296–301, (2013).
[15] L. Chen, X. Chen, Y. Liu, Y. Zhao, X. Zhang, *Journal of Semiconductor*, **38**, 054005, (2017).
[16] S.Vallisree, R.Thangavel, T. R. Lenkab , *Materials Research Express*, **6, No. 2,** (2018).
[17] X Li, A. Kanevce, J. V. Li, I, Repins, B. Egaas, R. Nouf. 2009 34th IEEE Photovoltaic Specialists Conference (PVSC), (2009).
[18] N. Touafek, R. Mahamdi, *International Journal of Renewable Energy Research*, **4, No.4**, 958-964 (2014).
[19] K. E. Knutsen, R. Schifano, E. S. Marstein, B. G. Svensson, A. Yu. Kuznetsov, *Phys. Status Solidi A*, **210, No. 3**, 585–588. (2013).
[20] A.Singh, A. Vij, D. Kumar, P. K. Khanna, M. Kumar, S. Gautam, K. H. Chae, *Semiconductor Science and Technology*, **28, No 2**, 025004, (2013).
[21] A. Rawat, M. Sharma, D. Chaudhary, S.Sudhakar, S. Kumar, *Solar Energy*, **110**, 691-703, (2014).